

Leading-order hadronic contributions to $g_\mu - 2$

Budapest-Marseille-Wuppertal Collaboration

Eric B. Gregory^{*1}, Zoltan Fodor^{1,2,3}, Christian Hoelbling¹, Stefan Krieg^{1,2}, Laurent Lellouch^{4,5}, Rehan Malak^{4,5,6}, Craig McNeile¹, Kalman Szabo⁷

¹*Department of Physics, Bergische Universität Wuppertal, Gausstr. 20, D-42119 Wuppertal, Germany*

²*IAS/JSC, Forschungszentrum Jülich, D-52425 Jülich, Germany*

³*Inst. for Theor. Physics, Eötvös University, Pázmány P. sét. 1/A, H-1117 Budapest, Hungary*

⁴*Aix-Marseille Université, CNRS, CPT, UMR 7332, F-13288 Marseille, France*

⁵*Université de Toulon, CNRS, CPT, UMR 7332, F-83957 La Garde, France*

⁶*CNRS, CEA, Maison de la Simulation, USR 3441, F-91191 Gif-sur-Yvette Cedex, France*

⁷*University of Regensburg, Universitätsstr. 31, 93053 Regensburg*

E-mail: gregory@uni-wuppertal.de

We present preliminary lattice results for the leading-order hadronic contribution to the muon anomalous magnetic moment, calculated with HEX-smearred clover fermions. In our calculation we include 2+1-flavor ensembles with pions at the physical mass.

31st International Symposium on Lattice Field Theory - LATTICE 2013

July 29 - August 3, 2013

Mainz, Germany

^{*}Speaker.

1. Introduction

The muon anomalous magnetic moment is among the most precisely measured quantities in physics with $a_\mu \equiv \frac{(g_\mu - 2)}{2}$ determined experimentally to about 0.5 parts per million [1]. Theoretical calculations of Standard Model contributions to a_μ have similar precision. There currently exists tension between Standard Model and experimental determinations of 3.6 standard deviations [2]:

$$a_\mu^{\text{exp}} - a_\mu^{\text{SM}} = 287(63)(49) \times 10^{-11}. \quad (1.1)$$

The possibility that this tension is a hint of beyond Standard Model physics has led to renewed effort to improve the precision of these determinations. The Muon $g - 2$ experiment at Fermilab aims to improve the experimental precision to 0.14 parts per million [3].

The full standard model calculation includes contributions from QED, electro-weak and hadronic processes. The uncertainty on the theory side is dominated by the calculation of the hadronic contributions. The current best precision of the leading such contribution, known as the hadronic vacuum polarization (HVP) contribution, comes from experimental e^+e^- cross-section data [5, 4] and $\tau \rightarrow \nu_\tau + \text{hadrons}$ decay data [6].

The challenge is for lattice QCD to provide first-principle calculations of the hadronic contributions to a_μ that meet or exceed the current precision of semi-empirical methods. There have been a number of attempts by different lattice groups [7, 8, 9, 10, 11] demonstrating the feasibility of the approach. A full calculation will require a calculation of the hadronic vacuum polarization (HVP), including disconnected contributions, as well as the contribution of light-by-light scattering through hadrons.

Here we give a preliminary report of our efforts to calculate the leading-order contribution of the HVP. We present results based on lattices with either 2+1 flavors or four non-degenerate flavors of HEX-smearred clover-type fermions. We include ensembles with pion masses at or below the physical value.

2. Lattice calculation

Our preliminary calculations have been performed on the ensembles listed in Table 1. We use HEX-smearred clover-type fermions. We use either two or three levels of HEX smearing. The “2-HEX” ensembles have $N_f = 2 + 1$ flavors and are described more fully in [12]. These include ensembles with the pion mass at or below the physical value. The “3-HEX” lattices have four non-degenerate flavors of dynamical fermions, corresponding to u , d , s and c quarks.

The contribution of the HVP at the lowest order comes from diagrams such as Fig. 1. The lattice method devised by Blum [13] is based on the recognition that these diagrams can be calculated by determining the vacuum-subtracted HVP, $\hat{\Pi}(Q^2)$ as a function of the square of the Euclidean momentum Q , then integrating [14]

$$a_\mu^{\text{had,LO}} = \frac{\alpha}{\pi} \int_0^\infty dQ^2 f(Q^2) \hat{\Pi}(Q^2), \quad (2.1)$$

with the kernel function

$$f(Q^2) = \frac{m_\mu^2 Q^2 Z(Q^2)^3 (1 - Q^2 Z(Q^2))}{1 + m_\mu^2 Q^2 Z(Q^2)^2}, \quad (2.2)$$

2-HEX ($N_f = 2 + 1$)						
am_{ud}^{bare}	am_s^{bare}	volume	# cfs	M_π (GeV)	n_{tw}	
$\beta = 3.31, a^{-1} = 1.697 \text{ GeV}$						
-0.09933	-0.0400	$48^3 \times 48$	928	0.136(2)		
-0.09300	-0.0400	$24^3 \times 48$	210	0.255(2)		
$\beta = 3.5, a^{-1} = 2.131 \text{ GeV}$						
-0.05294	-0.0060	$64^3 \times 64$	83	0.130(2)		
-0.04900	-0.0120	$32^3 \times 64$	216	0.250(2)		
-0.04900	-0.0060	$32^3 \times 64$	110	0.258(2)		
-0.04630	-0.0120	$32^3 \times 64$	212	0.308(2)		
$\beta = 3.61, a^{-1} = 2.561 \text{ GeV}$						
-0.03000	-0.0042	$32^3 \times 48$	188	0.332(4)	0.5, 0.25, 0.1	
$\beta = 3.7, a^{-1} = 3.026 \text{ GeV}$						
-0.02700	0.0000	$64^3 \times 64$	208	0.182(2)		
3-HEX ($N_f = 4$)						
am_u^{bare}	am_d^{bare}	am_s^{bare}	am_c^{bare}	volume	# cfs	M_π (GeV)
$\beta = 3.2, a^{-1} = 1.897 \text{ GeV}$						
-0.0806	-0.0794	-0.033	0.71	$32^3 \times 64$	240	0.250

Table 1: Configurations used in preliminary study.**Figure 1:** Leading-order connected and disconnected hadronic contributions to a_μ .

where

$$Z = -\frac{Q^2 - \sqrt{Q^4 + 4m_\mu^2 Q^2}}{2m_\mu^2 Q^2}. \quad (2.3)$$

On the lattice we calculate for each flavor, f , the HVP tensor as the Fourier transform of the vector current correlator:

$$\Pi_{\mu\nu}^f(\hat{Q}) = a^4 \sum_y e^{iQ(x + \frac{a\hat{\mu}}{2} - y)} \langle J_\mu^{\text{CVC}}(x) J_\nu^{\text{loc}}(y) \rangle, \quad (2.4)$$

with

$$J_\nu^{\text{loc},f}(y) = \bar{\psi}^f(x) \gamma_\nu \psi^f(x), \quad (2.5)$$

and the conserved vector current (CVC) as given by

$$J_\mu^{\text{CVC},f}(x) = \frac{1}{2} \left[\bar{\psi}^f(x + a\hat{\mu})(1 + \gamma_\mu) U_\mu^\dagger(x) \psi^f(x) - \bar{\psi}^f(x)(1 - \gamma_\mu) U_\mu(x) \psi^f(x + a\hat{\mu}) \right]. \quad (2.6)$$

The HVP tensor satisfies the Ward-Takahashi Identity (WTI) on the conserved index μ :

$$\hat{Q}_\mu \hat{\Pi}_{\mu\nu}^f = 0, \quad (2.7)$$

with the modified lattice momentum

$$\hat{Q}_\mu = \frac{2}{a} \sin\left(\frac{aQ_\mu}{2}\right) \quad \text{and} \quad Q_\mu = \frac{2\pi n_\mu}{L_\mu}. \quad (2.8)$$

To enforce conservation on the local current sink index ν we require $Q_\nu = 0$. We also use diagonal $\mu = \nu$ elements only.

With Euclidean momentum Q_μ , the vacuum-subtracted HVP scalar $\hat{\Pi}(Q^2)$ appearing in (2.1) is related to the HVP tensor $\Pi_{\mu\nu}^f(Q)$ through

$$\Pi_{\mu\nu}^f(Q) = (Q^2 \delta_{\mu\nu} - Q_\mu Q_\nu) \Pi^f(Q^2) \quad (2.9)$$

and

$$\hat{\Pi}(Q^2) = 4\pi\alpha \sum_{f=0}^{N_f} q_f^2 (\Pi^f(Q^2) - \Pi^f(0)), \quad (2.10)$$

where q_f is the electromagnetic charge of quark flavor f .

To perform the vacuum subtraction in (2.10) we must know the value of $\Pi^f(0)$, which is not directly accessible from the lattice data. To do so we fit the measured values of $\Pi^f(Q^2)$ to a suitable function of Q^2 and extrapolate to $Q^2 = 0$. For simplicity in this preliminary work we fit to:

$$\Pi(Q^2) = c + \sum_{i=0}^N \frac{b_i}{Q^2 + c_i}, \quad (2.11)$$

a multi-vector-dominance model, with $N = 1$ or 2 , as the data support. Golterman *et al.*[15] note in these proceedings that this is not an optimal fit ansatz. In the final calculation we will explore different fit forms to constrain systematic errors.

An example of the fits to unsubtracted HVP scalars is shown in Fig. 2. The vector dominance model suggests that the HVP scalar should behave approximately as

$$\Pi^{\text{tree}}(Q^2) = \frac{2}{3} \frac{f_V^2}{Q^2 + m_V^2}. \quad (2.12)$$

As a consistency check we compare values of M_ρ and f_ρ obtained from the fits ($M_\rho^{\text{HVP}} \equiv c_0^{1/2}$ and $f_\rho^{\text{HVP}} \equiv \sqrt{3b_0/2}$) respectively with those extracted from straightforward spectroscopy fits of the zero-momentum correlators. These comparisons are shown in Figs. 3a and 3b.

To determine $a_\mu^{\text{had,LO}}$ we use the fitted parameters to define a continuous function $\Pi(Q^2)$ with (2.11), substitute the resulting $\hat{\Pi}(Q^2)$ into the integral (2.1), which we evaluate numerically.

2.1 Twisted boundary conditions

The integrand $f(Q^2)\hat{\Pi}(Q^2)$ has a peak at around the muon mass, which is approximately an order of magnitude lower than the smallest, non-vanishing lattice momentum available on our lattices. This creates a large model-dependence as we extrapolate our results toward $Q^2 = 0$.

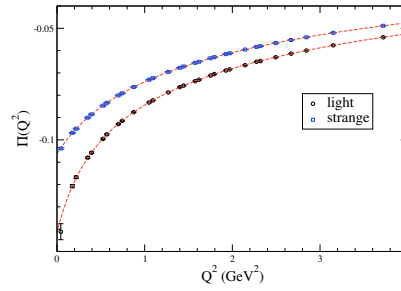


Figure 2: Sample fit of light and strange components of the HVP scalar from $\beta = 3.50$ $M_\pi = 250$ MeV data set.

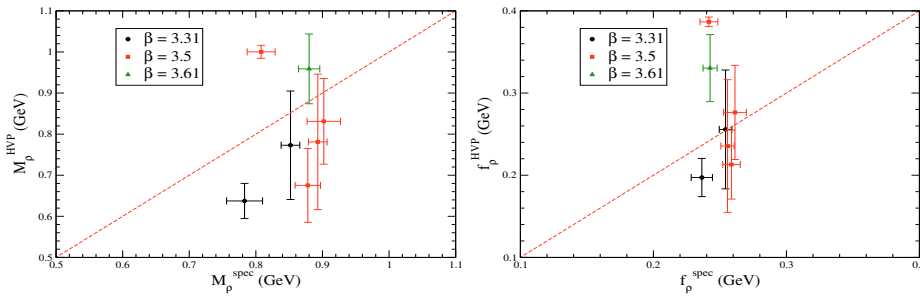


Figure 3: Comparison of M_ρ and f_ρ from HVP fits and spectroscopy fits.

Twisted boundary conditions have been proposed [16] as a method of accessing arbitrarily low lattice momenta. One must twist the spatial boundary conditions in the valence quark and anti-quark fields by a relative angle

$$\psi(x + L_\mu) = e^{i\theta_\mu^{\text{tw}}} \psi(x) \quad \text{with} \quad \theta_\mu^{\text{tw}} = 2\pi n_\mu^{\text{tw}}. \quad (2.13)$$

The lattice momenta transform as

$$Q_\mu \rightarrow Q_\mu - \theta_\mu^{\text{tw}}/L_\mu \quad (2.14)$$

in the twisted direction(s).

We explore this (Fig. 4) and note several issues. First, the naive twisting breaks the WTI, though the violation becomes negligible as the spatial volume increases. Aubin *et al.* [17] note this and provide a term to correct it. Second, the relative statistical error on $\hat{\Pi}(Q^2)$ grows approximately like $1/Q^4$ at low Q^2 due to the division by $(Q^2\delta_{\mu\nu} - Q_\mu Q_\nu)$ and the subsequent subtraction of the $Q^2 = 0$ value. At our current statistics, the new twisted points serve mainly as a consistency check without constraining the fit function significantly. We have not included twisted BC data in the preliminary results in the next section.

2.2 Matching to perturbation theory

A careful calculation of $a_\mu^{\text{had,LO}}$ should include a matching of lattice data to perturbation theory at large values of Q^2 . In Fig. 4b we demonstrate that such matching is feasible for the $Q^2 \approx 2$ GeV region, using expressions from [18]. We do not include such a matching in our current calculation, introducing systematic error of $\sim 1\%$ or less.

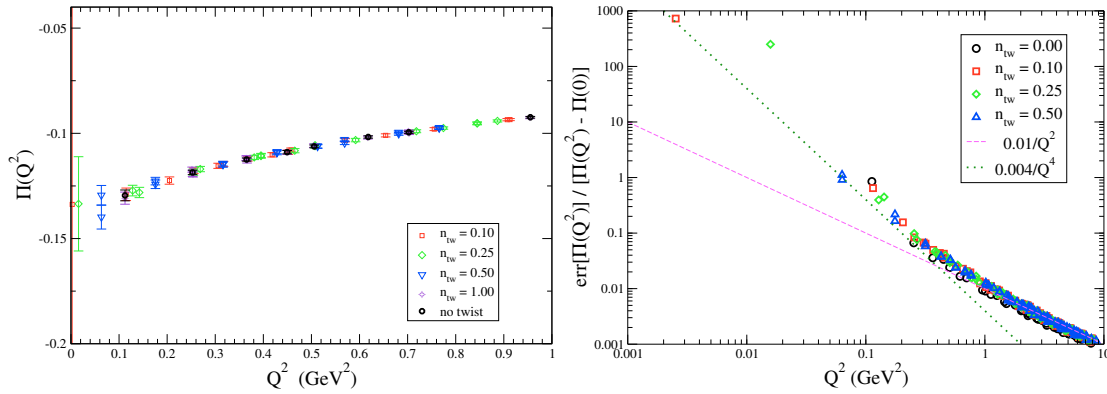


Figure 4: (left) Comparison of twisted BC and non-twisted BC data for the light quark channel of the $\beta = 3.61$ $M_\pi = 332$ MeV ensemble. (right) Error/signal for the same points. Dashed lines to guide the eye.

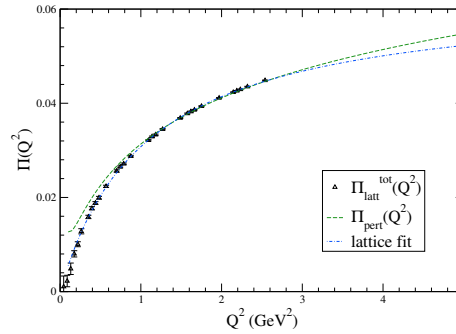


Figure 5: A sample matching of the lattice data to perturbation theory for $\beta = 3.5$, $M_\pi = 130$ MeV.

3. Results and conclusions

In Figs. 6a and 6b we display our preliminary results with statistical error bars only. Fig. 6a shows the value of $a_\mu^{\text{had,LO}}$ we obtain for the various ensembles, as a function of M_π^2 . We show results from some other groups for comparison. Figure 6b shows only our physical M_π ensemble results with other determinations (including calculations with experimental input).

Our future work will refine these calculations, with more ensembles, higher statistics and a full error budget. We also plan to include an estimate of the disconnected contribution.

4. Acknowledgments

The authors thank the Gauss Centre for Supercomputing (GCS) for providing computing time through the John von Neumann Institute for Computing (NIC) on the GCS share of the supercomputer JUQUEEN at Jülich Supercomputing Centre (JSC) and time granted on JUROPA at JSC. Computations were also performed using HPC resources provided by GENCI-[IDRIS] (grant 52275). This work was supported in part by the OCEVU Labex (ANR-11-LABX-0060) and the A*MIDEX project (ANR-11-IDEX-0001-02) funded by the “Investissements d’Avenir” French government program managed by the ANR. This work was in part funded by the “Deutsche Forschungsgemeinschaft” under the grant SFB-TR55.

References

- [1] G. W. Bennett *et al.* [Muon G-2 Collaboration], Phys. Rev. D **73**, 072003 (2006) [hep-ex/0602035].

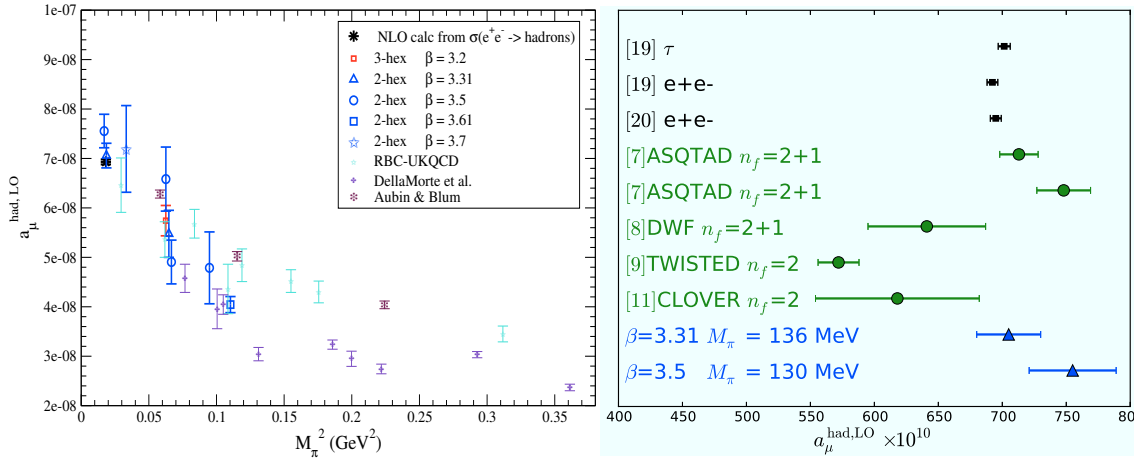


Figure 6: Figure *a* (left) our results for $a_\mu^{\text{had, LO}}$ obtained from the various ensembles, as a function of M_π^2 , together with those from other groups [7, 11, 8]. In Figure *b* (right) we compare the preliminary results from our two physical M_π point simulations (blue triangles) with those from (black squares) τ decay and e^+e^- cross-section data [19, 20] and from other lattice computations (green circles): [7, 8, 9, 11].

- [2] J. Beringer *et al.* (Particle Data Group), Phys. Rev. D **86**, 010001 (2012).
- [3] <http://muon-g-2.fnal.gov/>.
- [4] K. Hagiwara, *et al.*, JPHGB **G38**, 085003 (2011).
- [5] M. Davier, *et al.*, Eur. Phys. J. **C66**, 127 (2010). M. Davier, *et al.*, Eur. Phys. J. **C71**, 1515 (2011).
- [6] R. Alemany, *et al.*, Eur. Phys. J. **C2**, 123 (1998).
- [7] C. Aubin and T. Blum, Phys. Rev. D **75**, 114502 (2007) [hep-lat/0608011].
- [8] P. Boyle, *et al.* Phys. Rev. D **85**, 074504 (2012) [arXiv:1107.1497].
- [9] X. Feng, *et al.*, Nucl. Phys. Proc. Suppl. **225-227**, 269 (2012) [arXiv:1112.4946].
- [10] M. Gockeler *et al.* [QCDSF Collaboration], Nucl. Phys. B **688**, 135 (2004) [hep-lat/0312032].
- [11] M. Della Morte, *et al.* PoS LATTICE **2012**, 175 (2012) [arXiv:1211.1159].
- [12] S. Durr, *et al.*, JHEP **1108**, 148 (2011) [arXiv:1011.2711].
- [13] T. Blum, Phys. Rev. Lett. **91**, 052001 (2003) [hep-lat/0212018].
- [14] B. E. Lautrup, A. Peterman and E. de Rafael, Phys. Rept. **3** (1972) 193. B. E. Lautrup, A. Peterman and E. de Rafael, Nuovo Cim. A **1** (1971) 238.
- [15] M. Golterman, K. Maltman and S. Peris, [arXiv:1310.5928].
- [16] C. T. Sachrajda and G. Villadoro, Phys. Lett. B **609**, 73 (2005) [hep-lat/0411033].
- [17] C. Aubin, T. Blum, M. Golterman and S. Peris, Phys. Rev. D **88**, 074505 (2013) [arXiv:1307.4701].
- [18] K. G. Chetyrkin, J. H. Kuhn and M. Steinhauser, Nucl. Phys. B **482**, 213 (1996) [hep-ph/9606230].
- [19] M. Davier, *et al.*, Eur. Phys. J. C **71**, 1515 (2011) [arXiv:1010.4180].
- [20] K. Hagiwara, *et al.*, J. Phys. G **38**, 085003 (2011) [arXiv:1105.3149].